Termination layer dependence of Schottky barrier height for $La_{0.6}Sr_{0.4}MnO_3$/Nb:$SrTiO_3$ heterojunctions

M. Minohara,[1] R. Yasuhara,[1] H. Kumigashira,[1,2,3,*] and M. Oshima[1,2,4]

[1]*Department of Applied Chemistry, The University of Tokyo, 7-3-1 Hongo, Bunkyo-ku, Tokyo 113-8656, Japan*

[2]*Precursory Research for Embryonic Science and Technology (PRESTO), Japan Science and Technology Agency, Kawaguchi, Saitama 332-0012, Japan*

[3]*Synchrotron Radiation Research Organization, The University of Tokyo, Bunkyo-ku, Tokyo 113-8656, Japan*

[4]*Core Research for Evolutional Science and Technology (CREST), Japan Science and Technology Agency, Chiyoda-ku, Tokyo 102-0075, Japan*

(Received 27 January 2010; revised manuscript received 28 May 2010; published 21 June 2010)

We have investigated the interfacial termination layer dependence of the Schottky barrier height (SBH) for heterojunctions between polar $La_{0.6}Sr_{0.4}MnO_3$ (LSMO) and nonpolar Nb-doped $SrTiO_3$ (Nb:STO). The SBH for LSMO/TiO_2-Nb:STO is *higher* than the SBH predicted from the Schottky-Mott rule by 0.5 eV, indicating the formation of an interface dipole. In contrast, for LSMO/SrO-Nb:STO, the SBH is *lower* than that predicted from the Schottky-Mott rule by 0.4 eV. These results indicate that a change in the polarity of the polar LSMO overlayers results in inversion of the direction of the interface dipole. The modulation of SBH depending on the interfacial termination layer is reasonably explained by interfacial electronic reconstruction to prevent polar divergence.

DOI: 10.1103/PhysRevB.81.235322 PACS number(s): 73.30.+y, 73.20.−r, 73.90.+f, 79.60.Jv

Heterojunctions based on perovskite oxides, which have a chemical formula of ABO_3, have attracted considerable attention because of their potential applications to future electronic devices with multifunctional and highly stimulus-sensitive properties.[1–3] Extensive studies on the behavior of oxide heterojunctions have revealed that the properties of perovskite oxide devices can be tuned through interface effects such as spin exchange interactions,[4] charge transfer,[5–8] and band lineups.[9–11] However, in the design of these oxide devices, a fundamental question arises as to whether these interfaces can be described by an analogy to junction based on conventional semiconductors and/or metals at the starting point. A particularly interesting aspect of oxide heterojunctions is the appearance of metallic conductivities at the interface between band insulators depending on the terminating layer at the interface.[12,13]

The Schottky barrier height (SBH) formed at a metal/semiconductor perovskite oxide heterojunction is a parameter that dominates the characteristics of devices with such heterojunctions. Recently, it was reported that the SBH between a half-metallic ferromagnet $La_{0.6}Sr_{0.4}MnO_3$ (LSMO) and an *n*-type semiconductor Nb-doped $SrTiO_3$ (Nb:STO) is much higher than that predicted by the Schottky-Mott rule owing to the formation of an "interface dipole" at the heterojunction interface.[9–11] Since an interface dipole is formed only in the case of a polar/nonpolar perovskite oxide heterojunction,[9] it is reasonable to conclude that the interface dipole is correlated with an interfacial structure having polar discontinuity.[9,10,13] A perovskite oxide heterojunction ($ABO_3/A'B'O_3$) grown in the [001] direction has two types of interfacial structures, one having an $AO/BO_2 \| A'O/B'O_2$ layer sequence and another having a $BO_2/AO \| B'O_2/A'O$ layer sequence. Thus, different interfacial electronic structures emerge depending on the interfacial termination layer.[12] In the case of polar/nonpolar LSMO/Nb:STO Schottky junctions, potential modulation across the interface can be expected as a result of interfacial electronic reconstruction induced by polarity inversion of the LSMO layer concomitant with alternation of the terminating layer. Therefore, elucidation and modeling of the termination layer dependence of the SBH are essential not only for designing oxide devices with predetermined properties but also for understanding the interfacial electronic structure of oxide heterostructures.

In this study, we investigated the interfacial termination layer dependence of the SBH for polar/nonpolar LSMO/Nb:STO heterojunctions. As mentioned above, an LSMO/STO interface has two types of interfacial structures. These structures have the following stacking sequences: -MnO_2-$La_{0.6}Sr_{0.4}O$-TiO_2-SrO- (*n* type) and -$La_{0.6}Sr_{0.4}O$-MnO_2-SrO-TiO_2- (*p* type) [shown in the right panels of Figs. 1(a) and 1(b), respectively]. The band diagrams of two LSMO/Nb:STO heterojunctions having different interfacial termination layers were precisely determined by *in situ* photoemission spectroscopy (PES). The value of the interface dipole was estimated to be 0.5 eV for the *n*-type interface and −0.4 eV for the *p*-type interface. From these results, we conclude that the inversion of the polarity of the LSMO film due to a change in the termination layer at the interface results in inversion of the direction of the interface dipole. In this paper, we report on the interfacial termination layer dependence of the SBH and we discuss the origin of the change in SBH depending on the interfacial termination layer in terms of the electronic reconstruction that is characteristic of the polar/nonpolar interface.

LSMO/Nb:STO heterostructures with an *n*-type and *p*-type interface were fabricated on Nb-doped (0.05 wt %) STO (001) substrates in a laser molecular beam epitaxy chamber connected to a photoemission system at the beamline BL-2C of the Photon Factory in KEK.[14] Sintered LSMO and SrO_2 pellets were used as targets. The wet-etched TiO_2-terminated Nb:STO substrates were annealed at 1050 °C under an oxygen pressure of 1×10^{-7} Torr to ob-

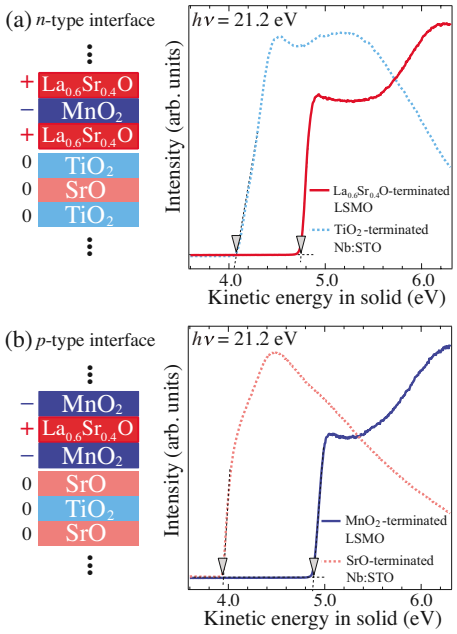

FIG. 1. (Color online) Schematic illustration of (a) *n*-type and (b) *p*-type LSMO/Nb:STO interface with layer sequences of -MnO_2-$La_{0.6}Sr_{0.4}O$-TiO_2-SrO- and -$La_{0.6}Sr_{0.4}O$-MnO_2-SrO-TiO_2-, respectively. The secondary electron emission spectra of the surfaces joined to each other at the interface are shown in the right panel. The thicknesses of LSMO films are about 20 ML (8 nm). The kinetic energy was calibrated by the Fermi level (E_F) of a gold film so that zero energy corresponds to E_F in each surfaces.

tain atomically flat substrates.[14] An LSMO/Nb:STO heterostructure with a *p*-type interface was fabricated by initially depositing one SrO atomic layer on the TiO_2-terminated Nb:STO substrate to change its termination from a TiO_2 layer to a SrO layer.[12,15,16] During subsequent LSMO depositions, the substrate was kept at a temperature of 1000 °C, and the ambient oxygen pressure was maintained at 1×10^{-4} Torr.[14] The thickness of the LSMO films was controlled on an atomic scale by monitoring the intensity oscillations of the reflection high-energy electron diffraction specular spot during film growth.[15–17] Samples (LSMO/Nb:STO heterostructures and Nb:STO substrates) were subsequently annealed at 400 °C for 45 min and under atmospheric pressure of oxygen to fill residual oxygen vacancies. After post annealing, the samples were moved into the photoemission chamber under a vacuum of 10^{-10} Torr. In-vacuum transfer is necessary in order to prevent surface contamination because it can cause the work function to deviate from the intrinsic values.[9]

The PES spectra were recorded using a Scienta SES-100 electron energy analyzer with a total energy resolution of 150 meV in the 600–800 eV photon energy range. For precise determination of work functions (ϕ_m) and electron affinities (χ_i), the secondary electron emission data were recorded with the He I (21.2 eV) resonance line as an excitation source.[9] The Fermi levels of the samples were referred to a gold foil, which was in electrical contact with the sample. The formation of atomically flat surfaces and chemically abrupt interfaces was confirmed by *ex situ* atomic force microscopy and transmission electron microscopy, respectively. Alternation of surface termination layers was confirmed by measuring the angular dependence of core-level spectra.[15]

Figure 1 shows the photoemission spectra of the surfaces of termination layer controlled LSMO and STO at the onset of secondary electron emission under an applied bias voltage of 9.0 V. As illustrated in the left panel of Fig. 1, $La_{0.6}Sr_{0.4}O$-terminated LSMO is joined with TiO_2-terminated STO to form an *n*-type interface, while MnO_2-terminated LSMO is joined with SrO-terminated STO to form a *p*-type interface. Thus, corresponding surfaces for two types of interfaces were measured for precise estimation of the ideal SBH. As can be seen in the right panel of Fig. 1, the photoemission signal increases steeply as the kinetic energy of the electron in solid exceeds the work function (ϕ_m) of LSMO or the electron affinity (χ_i) of Nb:STO. The threshold energies can be determined from the leading edge position of the secondary electron emission; the leading edge position is defined as the point of intersection between the extrapolated slope and the background. The work functions are determined to be 4.73 ± 0.02 eV for the $La_{0.6}Sr_{0.4}O$-terminated LSMO surface and 4.87 ± 0.02 eV for the MnO_2-terminated LSMO surface; the electron affinities of Nb:STO substrates with TiO_2- and SrO-terminated surfaces are 4.08 ± 0.02 and 3.86 ± 0.02 eV, respectively.

The observed tendency that the work functions (the electron affinities) of BO_2-terminated surface are larger than those of *A*O-terminated counterparts is in good agreement with the prediction from the recent theoretical calculation based on first-principles density-functional theory.[18] According to the calculation,[18–20] the difference between two terminations is originated from the increment of *B*-O bond covalency near the surface. Since it is expected that the covalent bonding nature at the surface induces the complicated surface reconstruction and transformations, more detailed experiments on surface structures and theoretical studies are necessary for further addressing the difference in work functions (electron affinities).

In order to estimate the SBH from the Schottky-Mott rule (Φ_B^{SM}), we determined the valence band maximum (VBM) of Nb:STO with SrO- and TiO_2-terminated surfaces. The VBM values were determined by measuring the valence band spectra. The VBM of Nb:STO was 3.1 ± 0.1 eV for both SrO- and TiO_2-terminated surfaces. Since the band gap of STO is 3.2 eV at room temperature, the obtained VBM values indicate that Nb:STO is an *n*-type degenerate semiconductor and that a flat band is maintained at both surfaces.[9,21] Owing to the negligibly small energy difference between the Fermi level (E_F) and the conduction band minimum (CBM) in the degenerate semiconductor Nb:STO, the electron affinity of Nb:STO is almost equal to its work function. Thus, assuming that an ideal Schottky barrier is formed at the interface, Φ_B^{SM} can be determined as the difference between ϕ_m of LSMO and χ_i of Nb:STO. The estimated Φ_B^{SM} for the *n*-type and *p*-type LSMO/Nb:STO interfaces are 0.65 ± 0.05 and 1.01 ± 0.05 eV, respectively.

In general, the actual SBH (Φ_B^{Act}) is very sensitive to the interfacial electronic states, and consequently, Φ_B^{Act} can deviate from Φ_B^{SM}. In fact, in the case of LSMO/Nb:STO Schottky junctions, the formation of an interface dipole is

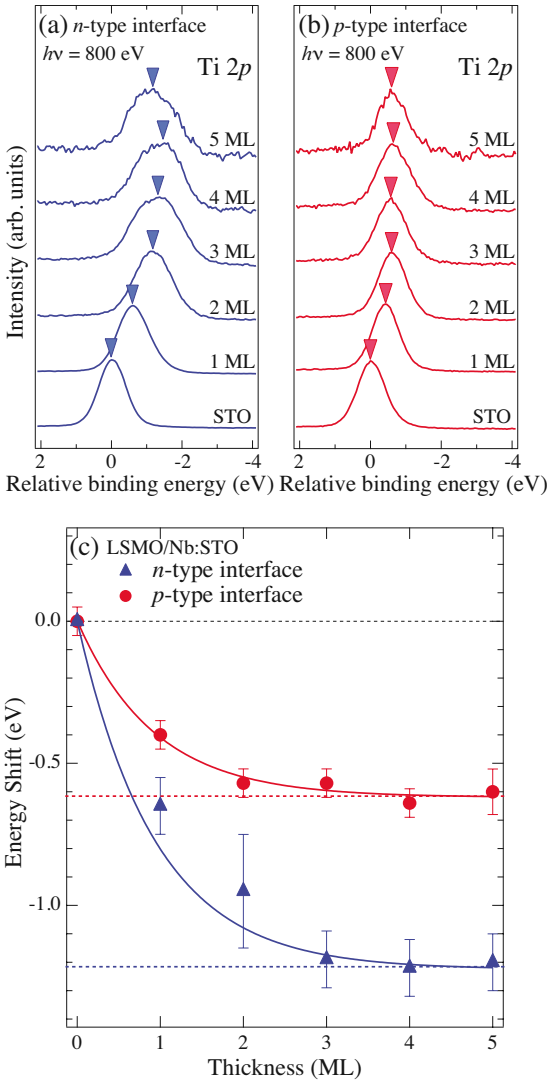

FIG. 2. (Color online) LSMO-overlayer-thickness dependence of Ti 2*p* core-level spectra of buried Nb:STO for (a) *n*-type and (b) *p*-type LSMO/Nb:STO heterojunctions. (c) Plot of the energy shift of the Ti 2*p* core-level peaks as a function of the LSMO overlayer thickness for *n*-type (triangle) and *p*-type (circle) heterojunctions. The lines serve as a guide for the eyes.

commonly observed; due to the interface dipole, Φ_B^{Act} is much higher than Φ_B^{SM}.[9–11] In order to determine the actual SBH directly, we have performed Ti 2*p* core-level PES measurements; the band bending caused by the deposition of a metallic oxide film on Nb:STO can be directly determined from the Ti 2*p* core-level shift. The results of the Ti 2*p* core-level PES measurements are shown in Fig. 2. It should be noted that the measurements reflect the band bending in the thin interface region on the Nb:STO side only, because of the short electron escape depth of 1–2 nm. For both junctions, a peak shift toward a lower binding energy is clearly observed with an increase in the thickness of the LSMO overlayer, indicating the formation of a Schottky barrier at the interface. Interestingly, the energy shifts due to band bending can be dramatically modulated by inserting one SrO atomic layer at the interface. Judging from the saturation level of the peak shift shown in Fig. 2(c), Φ_B^{Act} of the *n*-type and *p*-type

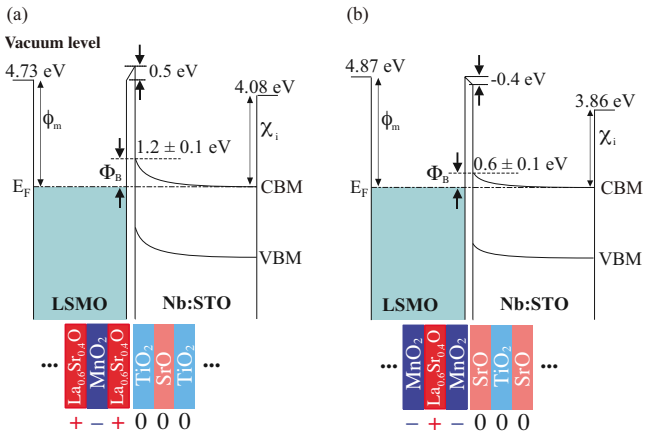

FIG. 3. (Color online) Band diagrams derived from the present *in situ* PES measurements for (a) *n*-type and (b) *p*-type LSMO/Nb:STO heterojunctions.

LSMO/Nb:STO heterojunctions can be estimated to be 1.2 ± 0.1 and 0.6 ± 0.1 eV, respectively.

In Fig. 2, it can be noticed that there is not only the energy shift due to band bending but also the significant broadening of core-level spectra with increasing the LSMO thickness. The peak width for the *n*-type interface is much broader than that for *p*-type interface. This broadening may be originated from the narrowing of depletion layer in the interface region, although the origin of the narrowing of depletion layer near the interface is not clear at a moment. It has been commonly observed that the SBH for manganites/TiO_2-terminated Nb:STO heterojunctions determined by PES measurements is much larger than that estimated by current-voltage (*I-V*) characteristics.[10,22] This difference may stem from the tunneling process in *I-V* measurements. Assuming the existence of a thin depletion layer with an abrupt potential drop near the interface, the tunneling current dominates the *I-V* characteristics rather than the thermionic emission current. The existence of a thin depletion layer at the interface may be in accordance with the significant broadenings of the Ti 2*p* core-level peak after LSMO deposition shown in Fig. 2(a). The possible potential modulation at the interface may complicate the peak assignments of Ti 2*p* core-level spectra. Thus, we use the centroid of Ti 2*p* core level as the peak position plotted in Fig. 2(c). Such peak assignments are a bit ambiguous. However, since the energy shift due to band bending is significantly larger than the uncertainty of peak-position assignments, our analysis is meaningful to obtain the picture of band lineup.

The band diagrams of both LSMO/Nb:STO Schottky junctions, deduced from the present PES experiments, are illustrated in Fig. 3. It is found that Φ_B^{Act} of *n*-type LSMO/Nb:STO is *higher* than Φ_B^{SM} by 0.5 eV, which indicates the formation of an interface dipole.[9] In contrast, Φ_B^{Act} of *p*-type LSMO/Nb:STO is *lower* than Φ_B^{SM} by 0.4 eV. These results suggest that a change in the termination layer at the polar/nonpolar heterointerface results in inversion of the direction of the interface dipole. In other words, the SBH of LSMO/Nb:STO junctions is modulated by 0.6 eV as a result of the inversion of the interface dipole.

Modulation of the interface dipole by changing the inter-

facial termination was first reported by Hikita *et al.* for LSMO/$SrMnO_3$ (SMO)/Nb:STO junctions having equivalent interfacial structures to LSMO/SrO/Nb:STO junctions in the present study.[10] Through internal photoemission (IPE) measurements, they observed a systematic increment in the SBH in going from the *n*-type interface (LSMO/Nb:STO) to the *p*-type interface (LSMO/SMO/Nb:STO). For the *n*-type interface, the value of the interface dipole observed in the present study is in good agreement with the reported value; however, there is a significant difference between the observed and reported values of the interface dipole for the *p*-type interface.[10] The discrepancy can be reconciled by considering the differences between information obtained by PES and information obtained by IPE measurements: PES can be used to probe only the potential at the edge of the depletion layer formed on the Nb:STO side,[9] whereas IPE can be used to probe the potential difference between Nb:STO and LSMO in the interface region. Assuming the occurrence of a downward bending inside the manganite layer, the IPE measurements overestimate the value of the interface dipole.[23] Since the SMO behaves as a *p*-type semiconductor and the SMO/Nb:STO heterojunction consequently exhibits typical *p*-*n* junction characteristics,[24] there is a high possibility of the bands of the manganites bending downward at the interface. In fact, a shift of Mn 3*d* t_{2g} peak toward a higher binding energy was clearly observed in previous resonance PES studies on STO-capped LSMO films (at the STO/LSMO interface) with an increase in the thickness of the STO overlayer.[25] Since the peak shift reflects the band bending occurring inside the manganites only, it strongly suggests the existence of downward band bending at the interface on LSMO side.

Next, we discuss the origin of the interface dipole formation. It has been reported that at a polar/nonpolar heterointerface based on transition metal oxides, electronic reconstruction induced by charge transfer through the interface occurs for preventing potential divergence.[13] The possible electronically reconstructed interfaces for *n*-type and *p*-type LSMO/Nb:STO are illustrated in Figs. 4(a) and 4(b), respectively. Assuming a fully ionic charge assignment using the nominal valence for each atomic layer, the present interfaces have a polar discontinuity at the interface having charge density of $-0.6q/+0.6q/0q/0q$ for *n*-type interface and $+0.6q/-0.6q/0q/0q$ *p*-type interface. The stacking of the polar layers, which consist of alternating $\pm 0.6q$ charge sheets, on nonpolar STO produces a negative and positive electric field inside the polar layer for *n*-type interface and *p*-type interface, respectively. Divergence of electrostatic potential from the interface can be prevented by accommodation (release) of $0.3q$ charge in (from) the MnO_2 atomic layer adjacent to the interface in the case of an *n*-type (*p*-type) interface. Even after this charge compensation, a finite electrostatic potential remains inside the LSMO layer, which may correspond to the observed interface dipole. On the basis of the electronic reconstruction shown in Fig. 4, we calculate the interfacial static potential by assuming a simple capacitor structure of an LSMO layer with a dielectric constant of 30 (Ref. 10) and a charge carrier sheet distance of 0.19 nm (a half unit cell of LSMO). The interfacial static potential of the *n*-type and *p*-type interfaces are estimated to be +0.6 and −0.2 V, respectively. The estimated interfacial static potentials are in good agreement with the observed values of the interface dipole (0.5 eV for *n*-type and −0.4 eV for *p*-type LSMO/Nb:STO).

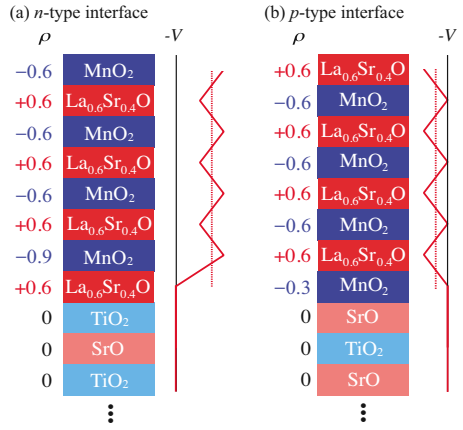

FIG. 4. (Color online) Possible electronic reconstruction and resultant electrostatic potential (thick solid line) for (a) *n*-type and (b) *p*-type LSMO/Nb:STO heterojunctions. The average of the static potential (thick dashed line) corresponds to the value of the interface dipole (see text for details).

The compensation of extra charges in the MnO_2 layer can be also naturally explained by taking into account the electronic configuration of Ti and Mn ions and the energy difference between the 3*d* levels of Ti and Mn ions.[25] By assuming a hypothetical single BO_2 layer, the electronic configuration is $t_{2g\uparrow}^0$ for Ti ions in a TiO_2 layer and $t_{2g\uparrow}^3 e_{g\uparrow}^0$ for Mn ions in a MnO_2 layer. When the electron-donor $La_{0.6}Sr_{0.4}O$ layer, which donates $0.6q$ per lattice site to the transition metal oxide layer, is shared by the MnO_2 and TiO_2 layers, the excess electrons are accommodated in the $e_{g\uparrow}$ states of Mn ions, owing to the energy difference of the 3*d* states in the transition metal ions. As a result, the effective electron concentration increases in a MnO_2 layer adjacent to the *n*-type interface. In contrast, the effective electron concentration decreases in a *p*-type interface owing to the alternation of the termination layer from an electron-donor $La_{0.6}Sr_{0.4}O$ layer to a SrO layer on the STO side. As a result, the charge redistribution illustrated in Fig. 4 is energetically favored from the viewpoint of the ionization energy of constituent transition metal, as well as the electrostatic potential discussed above. In fact, robust Ti^{4+} states and valence modulation in Mn ions at the LSMO/STO interface were clearly observed in previous PES measurements.[25]

Although the electronic reconstruction at the polar/nonpolar interface seems to reasonably explain the formation of the interface dipole, there remains the question about the validity of treating a conductive LSMO as an ionic insulator.[10] LSMO is a conductive oxide, and the interface dipole is subject to the metallic screening from carriers in an LSMO layer. The absence of metallic screening at the interface may be responsible for the insulating behavior of the LSMO layer in the interface region.[26–29] Recent studies on interfacial properties of LSMO layers have revealed that insulating transition layers with a thickness of about 4 ML exist at the LSMO/STO heterointerfaces.[26] A transition

LSMO layer is regarded as a nanocapacitor that is formed between metallic LSMO and semiconductive Nb:STO. Another possibility for the absence of metallic screening is the long screening length of the conduction carriers in LSMO.[10] Hikita *et al.* estimated the Thomas-Fermi screening length of LSMO to be about 0.31 nm, and they concluded that the length scale corresponds to a change in the valence of Mn at the first interface layer in simple ionic assignments. One of the key issues concerning transition metal oxides is the characteristic length scale at the interface where the complex physical properties manifest themselves. For an in-depth understanding of the origin of interface dipole formation, further investigation is necessary. In particular, it is important to clarify the effect of the charge density of the terminating layer on the SBH of the LSMO/STO interfaces.

Finally, we briefly discuss the potential divergence issue at the surface. Assuming that the same charge transfer occurs at the surface, the two different surface terminations of LSMO should have work functions differing by the same amount of 0.9 eV as the interface. However, the difference in work function of 0.14 ± 0.02 eV is much lower than that expected from electric reconstruction induced by charge transfer. Furthermore, the observed work functions of polar LSMO surface are close to those of nonpolar STO surface. These experimental facts strongly suggest that the surface of LSMO is not electronically equivalent to the interface: the divergence of electrostatic potential from the surface may be prevented not by charge transfer (electric reconstruction) but by structural reconstruction (atomic rearrangement) at the surface, since the energy cost of atomic rearrangement at the surface is much lower than that at the interface.[18] In order to understand the polarity issue at the surface, further investigations for surface structure of polar LSMO are necessary.

In conclusion, we have investigated the interfacial termination layer dependence of the Schottky barrier height (SBH) for heterojunctions between polar $La_{0.6}Sr_{0.4}MnO_3$ (LSMO) and nonpolar Nb-doped $SrTiO_3$ (Nb:STO) using *in situ* photoemission spectroscopy (PES). Insertion of one SrO atomic layer alters the interfacial structure of the LSMO/Nb:STO heterojunctions from -MnO_2-$La_{0.6}Sr_{0.4}O$-TiO_2-SrO- (*n* type) to -$La_{0.6}Sr_{0.4}O$-MnO_2-SrO-TiO_2- (*p* type), and consequently, the SBH is modulated from 1.2 ± 0.1 to 0.6 ± 0.1 eV. From the band diagram drawn from the *in situ* PES measurements, it is clear that SBH modulation occurs due to the formation of an interface dipole at the polar/nonpolar interface; the value of interface dipole for the *n*-type interface is 0.5 eV, while that for the *p*-type interface is −0.4 eV. These results indicate that inversion of interface dipole direction is a result of the inversion of polarity of the polar LSMO layers. The inversion of interface dipole direction is reasonably explained by interfacial electronic reconstruction to prevent polar divergence.

The authors are very grateful to Y. Hikita, H. Y. Hwang, and M. Lippmaa for the useful discussions. This work was supported by a Grant-in-Aid for Scientific Research (Grants No. A19684010 and No. A19204037) from the Japan Society for the Promotion of Science (JSPS) and JST PRESTO program. Two of the authors (M. M. and R. Y.) acknowledge the financial support from JSPS for Young Scientists.

*Author to whom correspondence should be addressed; kumigashira@sr.t.u-tokyo.ac.jp

[1] H. Yamada, Y. Ogawa, Y. Ishii, H. Sato, M. Kawasaki, H. Akoh, and Y. Tokura, Science **305**, 646 (2004).
[2] T. Fujii, M. Kawasaki, A. Sawa, Y. Kawazoe, H. Akoh, and Y. Tokura, Phys. Rev. B **75**, 165101 (2007).
[3] Y. Muraoka, T. Yamauchi, Y. Ueda, and Z. Hiroi, J. Phys.: Condens. Matter **14**, L757 (2002).
[4] M. Izumi, Y. Ogimoto, Y. Okimoto, T. Manako, P. Ahmet, K. Naka jima, T. Chikyow, M. Kawasaki, and Y. Tokura, Phys. Rev. B **64**, 064429 (2001).
[5] H. Kumigashira, D. Kobayashi, R. Hashimoto, A. Chikamatsu, M. Oshima, N. Nakagawa, T. Ohnishi, M. Lippmaa, H. Wadati, A. Fujimori, K. Ono, M. Kawasaki, and H. Koinuma, Appl. Phys. Lett. **84**, 5353 (2004).
[6] M. Izumi, Y. Murakami, Y. Konishi, T. Manako, M. Kawasaki, and Y. Tokura, Phys. Rev. B **60**, 1211 (1999).
[7] J. Chakhalian, J. W. Freeland, H.-U. Habermeier, G. Cristiani, G. Khaliullin, M. van Veenendaal, and B. Keimer, Science **318**, 1114 (2007).
[8] S. J. May, A. B. Shah, S. G. E. te Velthuis, M. R. Fitzsimmons, J. M. Zuo, X. Zhai, J. N. Eckstein, S. D. Bader, and A. Bhattacharya, Phys. Rev. B **77**, 174409 (2008).
[9] M. Minohara, I. Ohkubo, H. Kumigashira, and M. Oshima, Appl. Phys. Lett. **90**, 132123 (2007).
[10] Y. Hikita, M. Nishikawa, T. Ya jima, and H. Y. Hwang, Phys. Rev. B **79**, 073101 (2009).
[11] Z. Luo, J. Gao, A. B. Djurisic, C. T. Yip, and G. B. Zhang, Appl. Phys. Lett. **92**, 182501 (2008).
[12] A. Ohtomo and H. Y. Hwang, Nature (London) **427**, 423 (2004).
[13] N. Nakagawa, H. Y. Hwang, and D. A. Muller, Nature Mater. **5**, 204 (2006).
[14] K. Horiba, A. Chikamatsu, H. Kumigashira, M. Oshima, N. Nakagawa, M. Lippmaa, K. Ono, M. Kawasaki, and H. Koinuma, Phys. Rev. B **71**, 155420 (2005).
[15] H. Kumigashira, K. Horiba, H. Ohguchi, K. Ono, M. Oshima, N. Nakagawa, M. Lippmaa, M. Kawasaki, and H. Koinuma, Appl. Phys. Lett. **82**, 3430 (2003).
[16] K. Yoshimatsu, R. Yasuhara, H. Kumigashira, and M. Oshima, Phys. Rev. Lett. **101**, 026802 (2008).
[17] R. Takahashi, Y. Matsumoto, T. Ohsawa, M. Lippmaa, M. Kawasaki, and H. Koinuma, J. Cryst. Growth **234**, 505 (2002).
[18] M. Mrovec, J.-M. Albina, B. Meyer, and C. Elsässer, Phys. Rev. B **79**, 245121 (2009).
[19] E. Heifets, R. I. Eglitis, E. A. Kotomin, J. Maier, and G. Borstel, Phys. Rev. B **64**, 235417 (2001).
[20] E. Heifets, R. I. Eglitis, E. A. Kotomin, J. Maier, and G. Borstel, Surf. Sci. **513**, 211 (2002).
[21] K. Yoshimatsu, R. Yasuhara, H. Kumigashira, and M. Oshima, Phys. Rev. Lett. **102**, 199704 (2009).

[22] M. Minohara, Y. Furukawa, R. Yasuhara, H. Kumigashira, and M. Oshima, Appl. Phys. Lett. **94**, 242106 (2009).
[23] A. D. Wei, J. R. Sun, W. M. Lu, and B. G. Shen, Appl. Phys. Lett. **95**, 052502 (2009).
[24] A. Sawa, A. Yamamoto, H. Yamada, T. Fujii, M. Kawasaki, J. Matsuno, and Y. Tokura, Appl. Phys. Lett. **90**, 252102 (2007).
[25] H. Kumigashira, A. Chikamatsu, R. Hashimoto, M. Oshima, T. Ohnishi, M. Lippmaa, H. Wadati, A. Fujimori, K. Ono, M. Kawasaki, and H. Koinuma, Appl. Phys. Lett. **88**, 192504 (2006).
[26] K. Yoshimatsu, K. Horiba, H. Kumigashira, E. Ikenaga, and M. Oshima, Appl. Phys. Lett. **94**, 071901 (2009).
[27] A. Tebano, C. Aruta, S. Sanna, P. G. Medaglia, G. Balestrino, A. A. Sidorenko, R. D. Renzi, G. Ghiringhelli, L. Braicovich, V. Bisogni, and N. B. Brookes, Phys. Rev. Lett. **100**, 137401 (2008).
[28] M. Sahana, T. Walter, K. Dörr, K.-H. Müller, D. Eckert, and K. Brand, J. Appl. Phys. **89**, 6834 (2001).
[29] M. Huijben, L. W. Martin, Y.-H. Chu, M. B. Holcomb, P. Yu, G. Rijnders, D. H. A. Blank, and R. Ramesh, Phys. Rev. B **78**, 094413(R) (2008).